The Free Surface Turbulent Shear Layer[1]

G. T. CSANADY

Woods Hole Oceanographic Institution, Woods Hole, MA 02543

(Manuscript received 27 January 1983, in final form 20 July 1983)

ABSTRACT

In applying the wall layer analogy to a wind blown free surface it is necessary to decide in what coordinate system such an analogy is realistic. A smoothed sea surface is taken to be that produced by the nearly irrotational components of the wave field, relegating irregular, dissipative wavelets to turbulence. It is then possible to regard wave motion and shear flow as independent, except for the vortex force effect of Stokes drift, discussed by Leibovich. An analysis of the available observations shows that the free surface shear layer has many of the characteristics of the wall layer. A major difference is a much larger roughness parameter, arising presumably from direct energy input to surface turbulence by the wind. Velocity gradients near the free surface are much smaller than over a solid wall under otherwise comparable conditions.

1. Introduction

Wind stress acting upon the sea surface is commonly supposed to generate shear flow analogous to the turbulent boundary layer along a flat plate. This conceptual model underlies Ekman's (1905) classical memoir, the comprehensive analysis of the "layer of frictional influence" by Rossby and Montgomery (1935), and many later theoretical contributions, such as the recent analysis of a postulated constant stress layer by Madsen (1977). Given the chaotic and rapidly varying appearance of a wind-blown sea surface, however, it is not clear how precisely the boundary layer analogy should be applied, especially at depths of centimeters and decimeters. This analogy has, indeed, been questioned in the literature on several occasions. In two widely quoted contributions Bye (1965, 1967) at first analyzed his observations on the drift of surface floats in the framework of the boundary layer analogy, then, returning to the subject, suggested that the observed velocity distribution could also be ascribed to irrotational wave motion (Stokes drift).

Two fundamental issues arise in this controversy: 1) what measurement and averaging method, if any, will yield a mean flow structure analogous to the flat plate turbulent boundary layer, and in particular to the constant stress layer (wall layer); 2) if such a method can be found, in what manner and degree will the observed velocity distribution in a free surface shear layer differ from the wall layer. Will Karman's constant be the same? What will be the hydrodynamic roughness on the water side? Is it necessary to "correct" observations obtained with the aid of Lagrangian tracers by subtracting Stokes drift, as has been done, e.g., by Wu (1975) or Kenney (1977)?

Although past empirical studies of the free surface shear layer have given some implicit answers, these fundamental issues have not been systematically discussed previously. The purpose of the present note is to bring them into the open and to suggest their resolution.

2. The wall layer analogy

In a high sea state the sea surface is occupied by many sharp crested and breaking wavelets, whitecaps and foam and is clearly not a simple surface from which depth could be readily measured. In a lower sea state the small-scale irregularity of the surface motion is not as gross, but still considerable. Therefore, the first question that arises in connection with the wall layer analogy is, what smoothed version of the sea surface should serve as a $z = 0$ coordinate surface. The choice of the hydrostatic equilibrium level is, of course, not useful: one loses most of the shear layer between the main wind–wave crests and the troughs. One must decide what surface irregularities are to be regarded as "roughness" and imagined smoothed out, what others retained to make up a more regularly undulating surface. By what criteria should one make such a choice?

The geometrical objective of generating a suitably smooth mean coordinate surface is achieved by filtering out the sharp-crested irregularities (and disregarding foam and spray). Munk (1955) has given a schematic sketch of typical wavenumber spectra of elevation, slope and curvature, reproduced here as Fig. 1. The spectra of elevation and curvature do not overlap significantly, and are separated roughly by the wavenumber $k = 10\ \mathrm{m}^{-1}$. After filtering out shorter waves, the

[1] Woods Hole Oceanographic Institution Contribution No. 5227.

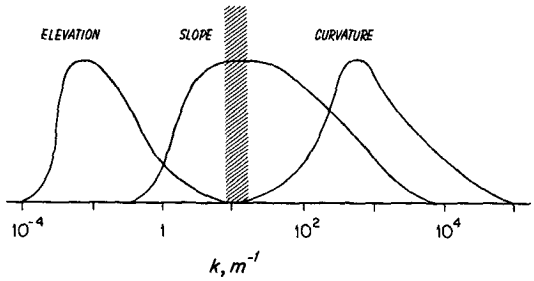

FIG. 1. Typical relationship of elevation, slope and curvature spectra against wavenumber k (m^{-1}). A slick dissipates wavelets to the right of the shaded band. From Munk (1955).

curvature of the remaining smoothed surface becomes quite small. The shaded vertical band was inserted into Fig. 1 by Munk to indicate the part of the spectrum dissipated by a surface slick. Conveniently a slick physically accomplishes the filtering operation needed conceptually for the application of the wall layer analogy to a natural (slickless) wind-blown surface.

There is a second consideration: the waves not filtered out should constitute the equivalent of the irrotational flow field outside a boundary layer. Otherwise, their vorticity and turbulence would interact with and compound the vorticity and turbulence generated by the shear flow and presumably affect the structure of the latter. Sharp crested and other rapidly decaying wavelets are presumably strongly vortical and should be filtered out and relegated to "turbulence". Because such turbulence exists independently of the shear flow (through energy input from the wind) it must be expected to affect the properties of the flow in the immediate neighborhood of the surface. The wall layer analogy can be expected to apply only at such depths where the shear flow-generated turbulence is much more intense than the wavelet turbulence, if such depths exist.

What wavelets are dissipative, and what others are more persistent, i.e., nearly irrotational, is difficult to decide on the basis of information on spectra alone. Dissipation is presumably linked to inertial motions in sharp-crested breaking wavelets, perhaps through a mechanism akin to that discussed by Longuet-Higgins and Turner (1974). The sea surface contains many such wavelets resulting in its wrinkled or "diamond-patterned" (Kinsman, 1965) appearance. A pair of stereo-photographs on pp. 332–333 of Neumann and Pierson (1966) illustrates the crescent-shaped wavelets involved, having sharp forward edges, and a typical wavelength of 0.3 m. A search of the literature has failed to turn up a zeroth-order, factual description of the structure and behavior of the high wavenumber (say, $k \geq 1$ m^{-1}) components of a wind-blown sea surface. In a footnote on p. 5 of Kinsman (1965) one finds a reference to "short, 'young' ripples" among "wave trains of many ages," illustrated by an excellent, sharp photograph on p. 4. However, the subject is not pursued either descriptively or analytically. The Appendix of the present paper has been transcribed from notes taken on a cruise in a following wind, when it was easy to observe the small scale wave motion. Such crude visual observations must have been made by many oceanographers.

However crude the visual evidence, one derives from it the observation that short-lived supposedly dissipative wavelets are those with a wavelength shorter than about a meter, i.e., $k \geq 6$ m^{-1}. This is not significantly different from the previously discussed cutoff for sharp crested wavelets at $k \approx 10$ m^{-1}.

A third important requirement for the validity of the wall layer analogy is that the horizontal force of the wind be exerted "at" the wall, either as shear stress or as form drag on the roughness elements. The conceptually filtered-out sharp-crested and dissipative wavelets are clearly the analogues of roughness elements. Any force exerted by the wind on these appears as Reynolds stress at a level below the deepest wavelet trough. The typical amplitude of these wavelets being less than 1 cm, one may expect the wall layer analogy to hold at a somewhat greater depth, provided that the waves not filtered out do not significantly affect the vertical momentum flux at these depths. If there is significant momentum transfer to or from waves longer than those filtered, and if those waves convert the momentum flux into Reynolds stress within the shear layer, then conditions within the latter differ from a constant stress layer. If, on the other hand, the longer waves use any such direct momentum gain or loss to increase or decrease their wave momentum, the shear layer remains unaffected.

Is it reasonable to suppose that a large fraction of the wind stress is transmitted by short wavelets, and that the longer waves do not significantly interfere with the Reynolds stress within a surface layer, say a meter or two thick? From studies of the air flow above a water surface it has for some time been clear that it is precisely the small wavelets that act as the principal roughness elements, transferring momentum mainly through form drag (Munk, 1955; Roll, 1965; Phillips, 1966; Wu, 1969; Kraus, 1972). Recent studies of Kondo *et al.* (1973) and Kawai (1981, 1982) have elucidated some details. The air flow separates from the crests of sharp-crested wavelets much as above solid roughness elements. The amplitude of the typical wavelet which acts in this manner is of order 1 cm. The average roughness size exceeds the thickness of the viscous sublayer on the air side at wind speeds in excess of 2 m s^{-1} while fully rough air flow, i.e., predominance of form drag over viscous stress, prevails in winds above 7 m s^{-1}. It is reasonable to identify the roughness elements acting *on the air flow* with the wrinkles and sharp-crested crescentic wavelets of the sea surface. Relegating all wavelets in the wavenumber range $k \geq 6$ m^{-1} to turbulence should insure that the

population of roughness elements acting on the air flow is included in what is regarded as roughness on the water side.

It is important to emphasize again that direct momentum transfer to or from the wind from or to the longer and larger nearly irrotational waves does not affect the validity of the wall layer analogy. However, were there dissipative waves of 0.3–1 m amplitude, they would convert their momentum gain into Reynolds stress at similar depths and change the character of the shear layer. In the final analysis, the wall layer analogy may be valid because the dissipative waves are known to have small amplitudes, and because these same small wavelets also extract considerable momentum from the air flow, partly on account of their sharp-crested shape. Whether the analogy is in fact valid, can of course only be decided by observation.

Nevertheless, some limitations of the wall layer analogy are already clear. Except in very light wind, or under an extensive slick, one should not expect to find a viscous sublayer. Under a natural wind-blown surface, at the moderate friction velocity of $u_* = 1$ cm s^{-1} (in water, wind speed 7 m s^{-1}) the sublayer, if it existed, and if it carried all the shear stress, would be about 1 mm thick. The representative amplitude of very short surface irregularities at this wind speed is, according to Kondo *et al.* (1973), about 4 mm, and the air flow is "fully rough," most momentum transfer being via form drag. Hence any viscous sublayer would carry only a fraction of the stress and be thinner still. Moreover, as in the case of a solid rough surface, the velocity distribution within the depth range of the roughness elements themselves is outside the scope of the simple parameterization known as the law of the wall.

3. Field observations using drifters and drogues

Can one devise a measuring technique to yield a mean velocity distribution below the smoothed sea surface, at depths of the order of centimeters and decimeters? Surface drifters followed for periods of the order of 10 min or more automatically provide average velocities. If they are also so constructed as to avoid bobbing up and down with the short wavelets, and if direct wind drag on them is negligible, they should respond to the mean velocities in question.

Bye (1965) seems to have been the first to carry out systematic field observations of the surface shear layer velocity distribution in this manner, in Lough Nead, Ireland. His floats were 2.5 cm square wooden rods, of varying length, weighted at one end so that the other end would barely break the surface. The longer rods were also fitted with a horizontal plate to prevent bobbing. In effect these rods were little spar buoys that filtered out high frequency up and down motions, but followed the longer waves. The longest rod used was 1 m.

In our own experiments in Cape Cod Bay and Lake Huron (Churchill and Csanady, 1983) "horsehair" drifters were used, 20 cm square, 2.5 to 20 cm deep. Horsehair is a synthetic elastic sponge, containing many thin fibers, but mostly void space, and the contact surface between the fibers and the water is large. Slabs of sponge, 2.5 to 20 cm thick, were made slightly buoyant by attaching to their top surface a thin buoyant layer. A 20 cm × 20 cm square slab so prepared floats with its top barely at the surface, and with small wavelets washing over it. Direct wind drag over the slab should therefore be negligible provided that the slab does not "tumble" in the waves. When tumbling, the sides or bottom of a drifter are exposed to wind drag, increasing its velocity. Large horsehair drifters (say a 1 m × 1 m slab) readily tumble, especially in stronger winds, and were found to travel faster than smaller ones. This limits the size of slabs useful in drifter studies.

On the other hand, drifters too small do not filter out the vertical motions associated with breaking wavelets and plunge to depths of order 0.1 m. That water particles plunge to such depths has been demonstrated in the laboratory by Donelan (1978). Plunging drifters average velocity over their range of plunging and travel more slowly than somewhat larger drifters. On some occasions of stronger winds a slab of horsehair only 2.5 cm thick was found to plunge, while a 5 cm one did not, with the result that the thicker slab traveled faster. Confetti or computer cards thrown on the surface were also found to plunge in brisk winds.

We have found 20 cm square horsehair drifters, 2.5 to 20 cm thick, effective for filtering out the small scale surface motion without plunging or tumbling.

Kenney (1977) has also reported observations of the surface shear layer velocity distribution in the Lake of the Woods. He used 10 cm deep, 50 cm wide drogues, centered at a number of depths, attached to small surface floats.

Detailed laboratory observations of the surface shear layer in wind–water tanks have also been carried out; see Shemdin (1972) and Wu (1975). Shemdin used small paper disks (like confetti) as tracers, and tried to eliminate the effects of bobbing motions by timing only those disks that remained at their original level. Wu used spherical surface floats of slight buoyancy, 0.05–0.6 cm in diameter, and triangular submerged floats 2.5 cm on the side (which acted as drogues) to 4 cm depth. The submerged floats were constructed similarly to Bye's rods with stabilizer plate and were resistant to bobbing. Because the water surface in laboratory experiments is presumably quite different from a natural wind blown surface, the laboratory data will not be discussed here in detail, and will only be used for qualitative comparisons with field observations.

One question arising in the interpretation of experiments with drifters (surface floats of finite depth) or drogues (resistance elements of finite depth, sus-

pended from a small surface float) is, at what level the velocity of the fluid equals that of the drifter or drogue. All investigators except Bye have supposed the mid-depth of the float or resistance element to be the relevant level, clearly a reasonable approximation for relatively shallow floats, given a modest curvature of the velocity distribution. Bye (1965), who used some quite deep floats, however, calculated the float velocity which results in zero net force on the float, using a quadratic drag law. The calculation is based on a logarithmic velocity distribution right up to the surface, including an integrable singularity where $\log z \to (-\infty)$, and grossly overestimates the influence of velocity profile curvature.

A typical observed velocity distribution exhibits only slight curvature and is well enough represented locally by a Taylor series expansion to second order. Using a linear drag law (presumably appropriate for the horsehair floats) one can show that the difference between the level where the fluid velocity equals float velocity (z_f) and the mid-depth of a float (or drogue element) (z_m) is

$$z_f - z_m = \frac{d^2}{24l}, \tag{1}$$

where d is float or drogue element depth and l is a length scale derived from the velocity profile:

$$l = \frac{du}{dz}\left(\frac{d^2u}{dz^2}\right)^{-1}. \tag{2}$$

According to this formula the error in velocity due to assigning float velocity to mid-depth is typically less than 0.1 cm s^{-1}, which is usually well within the accuracy of such observations. A quadratic law yields a not very different result. In the case of Bye's deepest float the error would have been slightly greater, although still less than that due to supposing float velocity equal to fluid velocity at 0.27 times float depth, as Bye has done. Even this somewhat unrealistic choice of equivalent float depth has, however, little influence on the general character of the observed velocity distribution: all of the conclusions to be arrived at below follow whether one uses Bye's data as he presented them, or corrected to a more reasonable equivalent float depth (although the calculated roughness length is *larger* if a better estimate of the equivalent float level z_f is used).

Another difficulty in this type of experiment is that the surface velocity u_s cannot be determined directly from the motion of finite depth drifters. However, visual observations of aluminum dust thrown on the surface, computer cards, natural debris, as well as of wetted confetti, when its motion can be followed, invariably show that, while there is a velocity gradient at the surface, this is not substantially different from the gradient at, say, 5 cm depth, where it can be fairly accurately inferred from the differential motion of, say, 5 cm and 10 cm thick slabs. In connection with various studies of surface layer diffusion (Csanady, 1963, 1970), windrows (Csanady, 1965, Csanady and Pade 1969) and of the drifter and drogue studies already referred to, we have many times tried to discover the equivalent of a viscous sublayer, or at least a strongly sheared layer at the surface. On a non-slick natural surface, under at least moderate winds, the attempt has invariably failed, and always evidently for the reason that the small wavelets rapidly and effectively stir the surface layer to at least a few centimeters depth.

Given the regular behavior of the velocity distribution near the free surface, the surface velocity is reasonably determined by extrapolation. Because an observed value can usually be assigned to the 2.5 cm depth, the error of such an extrapolation is likely to be small, probably of order one u_*. It is difficult to see by what other practical method a mean velocity could be assigned to a conceptually smoothed sea surface, which is actually covered by many irregular, transient roughness elements.

4. The problem of Stokes drift

A more difficult question is whether the second-order kinematic effects of the unfiltered (nearly irrotational) longer waves, which result in Stokes drift, in some way interfere with the wall layer analogy. One possibility is that vertical turbulent velocities transport total horizontal momentum, including wave momentum, i.e., Stokes drift. The distribution of the mass transport velocity near the free surface of a slightly viscous liquid has been extensively discussed in the literature (Longuet-Higgins, 1953, 1960; Pierson, 1962; Chang, 1969; Ünlüata and Mei, 1970; Madsen, 1978; Craik, 1982; Weber, 1983). The mass transport velocity u_L is defined as the sum of the Stokes velocity u_s and an induced Eulerian velocity u_E of the same order. The latter develops through a slow downward diffusion of vorticity, so that the resulting combined second order flow is able to satisfy various boundary conditions. However, as Craik (1982) points out, the calculated laminar velocity distributions are all unstable to spanwise disturbances and unlikely to be realized. One therefore expects the observed Eulerian second-order flow component to possess the character of turbulent shear flow. The question remains, whether or how vertical momentum transfer is affected by the gradient of Stokes drift: is the total Reynolds stress some eddy viscosity times $\partial/\partial z(u_E + u_s)$, $\partial u_E/\partial z$, or some intermediate value?

To answer this question, one notes that wave-orbital velocities are reestablished by the first order pressure field in a time period of order σ^{-1}. Hence, if u_* is the order of the typical vertical eddy velocity, the effective mixing length for Stokes drift is of order

$$l \sim u_*\sigma^{-1}.$$

The eddy vertical motion therefore carries a typical

momentum excess of $l(du_s/dz)$, and a Reynolds stress of order

$$\overline{u_s'w'} \sim u_*^2 \sigma^{-1} \frac{du_s}{dz}.$$

The nondimensional Stokes velocity gradient $\sigma^{-1}(du_s/dz)$ is of order ϵ^2 ($\epsilon = ak$, wave slope, a = wave amplitude) or small compared to unity. Hence the vertical momentum flux associated with the gradient of Stokes velocity is generally negligible compared to the total stress.

The interaction of irrotational wave motion, turbulent shear flow, and small-scale turbulence has been exhaustively discussed in a series of recent contributions related to the mechanics of Langmuir circulations by Craik (1970, 1977, 1982), Craik and Leibovich (1976), Leibovich (1977, 1980, 1983), and Leibovich and Paolucci (1980, 1981). From these contributions a clear conceptual framework has emerged to which the wall analogy is readily coupled. The key hypotheses of the Craik-Leibovich theory are:

1) The dominant water velocities near the free surface are the orbital motions in nearly irrotational waves. These are of order ϵc, where c is wave celerity, $c = \sigma k^{-1}$.

2) Velocities of the turbulent shear flow are of the same order as Stokes drift, i.e., of order $\epsilon^2 c$. Langmuir circulations arising in the cross-wind plane have similar characteristic velocities.

3) Small turbulent eddies are present and these act in a viscosity-like manner. Their time scale is short compared with the time scale σ^{-1} of the irrotational waves, which in turn is short compared to the advective time scale of the Langmuir circulations.

These hypotheses are in accord with known characteristics of the near-surface motion and are readily reconciled with the requirements of the wall layer analogy discussed earlier. The unfiltered longer waves may be supposed nearly irrotational giving rise to Stokes drift, while the breaking wavelets constitute short time-scale turbulence.

The various theoretical contributions cited above (especially Leibovich, 1977) clearly establish that the main dynamical interaction between the wave motion and the shear flow consists of a "vortex force" effect of the Stokes drift on the cross-wind vorticity of the shear flow. This results in a form of hydrodynamic instability not unlike the instability of a fluid cooled from above, and the generation of cross-wind Langmuir circulation cells. The down-wind shear flow is linearly superimposed on Stokes drift. The shear flow is also modified by the momentum advection associated with Langmuir circulation. The Langmuir cells act as large, wall-bound vortices and produce effects familiar from other wall layers, in particular a logarithmic velocity distribution, as was specifically demonstrated by Leibovich (1977).

Floats and drogues participate in the orbital motion of the long (unfiltered) waves by design and by hypothesis, and are therefore subject to Stokes drift. The simplest physical explanation of this kinematic effect is (Flierl, 1981) that water particles, or floats, follow a progressive wave when in the forward phase of the wave cycle, move against the wave in the backward phase. Thus they stay longer moving forward than backward. A key result of the careful theoretical analysis of Leibovich (1977) and the other cited papers is that the Stokes drift may be taken to be independent of the shear flow. Hence field observations must be corrected by subtracting Stokes drift, if it is desired to arrive at the underlying shear flow velocity distribution.

The result should be immediately qualified by noting that only the Stokes drift associated with the approximately irrotational longer waves should be so considered. A calculation of Stokes drift as a linear superposition of contributions weighted by the wave spectrum (such as that of Bye, 1967, or Kenyon, 1969) should certainly be cut off at a wave number beyond which the waves are sharp crested and dissipative. Even then it is not certain that such a spectral calculation of a second order effect is at all accurate. An equally reasonable estimate may be the calculation of Stokes drift of a single harmonic wave train, of a wavelength and frequency appropriate to the spectral peak, as has been used by Kenney (1977).

Although the Stokes drift and shear flow velocities are generally of the same order of magnitude, a realistic correction for Stokes drift only changes the surface velocity gradient moderately. The same applies to the velocity defect $u_s - u(z)$ at depths of 1 m and less. As with the correction for finite float depth, the conclusions relating to the character of the surface shear layer velocity distribution remain qualitatively unaffected whether the correction is made or not. Because in most cases it is doubtful what precise corrections should be applied, the observations will be discussed below without any attempt at corrections. The principal effect of this is that surface roughness on the water side is *un*derestimated (or that the near surface velocity gradient is overestimated).

5. Evidence for a "Surface Shear Layer"

It is now appropriate to examine the limited evidence available on the near surface velocity distribution and assess the validity of the wall layer analogy. The principal characteristic of a wall layer along a solid surface is shear aligned with the surface stress. Velocity vectors observed below a wind-blown free surface show the presence of a similar layer, called here the surface shear layer. The absolute velocity vectors near the surface may vary widely from case to case, according to what the velocity well below the shear layer happens to be. However, regardless of the direction of the deeper flow, within a surface layer a meter or two deep relative

motion is usually found to occur in a vertical plane parallel to the wind. Examples have been shown by Kenney (1977)—see Fig. 2 here—and by Churchill and Csanady (1983).

How close is the analogy between a surface shear layer and a wall layer? Consider the distribution of the along-wind velocity component in a frame of reference moving with the surface velocity. The velocity defect, $u_s - u(z)$, where u_s is downwind surface velocity, $u(z)$ the same velocity component at level z, has a distribution reminiscent of mean velocities in a pipe or boundary layer. The velocity gradient is a maximum at the wall and drops smoothly with distance from the surface.

In semilogarithmic coordinates the near-surface velocity distribution follows a straight line, over a certain range of depth. Over the corresponding range in a wall layer over a solid surface, one has

$$z\frac{du}{dz} = \frac{u_*}{\kappa}, \tag{4}$$

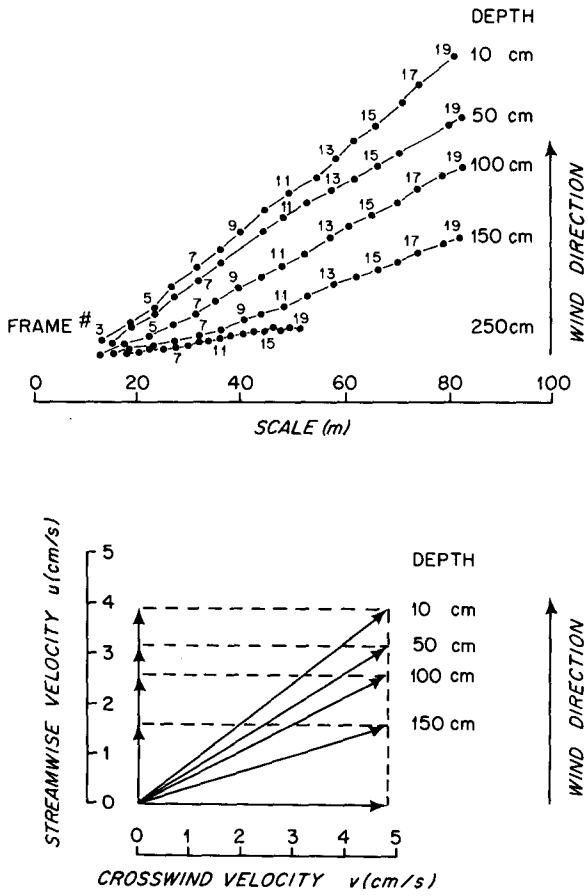

FIG. 2. Current velocity vectors observed by Kenney (1977) in the Lake of the Woods, 3 September 1974. Top: successive drogue positions; bottom: velocity vectors, and projections to along-wind and across-wind axis. The cross-wind component is constant, the along-wind components increase toward the surface.

where $u_* = (\tau_w/\rho)^{1/2}$ is the friction velocity, with τ_w wall stress, ρ fluid density, and $\kappa \approx 0.4$ is Karman's constant. A straight line in a semilogarithmic plot merely shows that the quantity on the left side of Eq. (4) is a constant, but not what the value of that constant is. However, if one supposes that the same relationship holds in the surface shear layer as in the wall layer, the friction velocity u_* may be determined from Eq. (4) (this is the "profile method" of surface stress determination). Two questions arise: does u_*, so determined, actually vary as $\tau_w^{1/2}$, and if so, is its magnitude correct, i.e., is Karman's constant the same as in a wall layer?

An independent estimate of the surface stress can be obtained from the wind velocity distribution above the water surface or from at least one wind speed, on the further supposition that most of the momentum is transferred by the wind to the small wavelets. This method generally yields much the same u_* as the profile method in water. At any rate, the scatter is not improved by changing the value of κ. To the limited accuracy of the existing evidence, it may be concluded that Eq. (4) holds on the water side of the air–sea interface with the same Karman's constant as on the air side or as in other wall layers. This conclusion was already reached by Bye (1965) and Kenney (1977) on the basis of field studies, and by Shemdin (1972) and Wu (1975) from laboratory work. The same law was furthermore found valid in turbulent flow along a liquid–liquid interface across which the density changes abruptly (Lofquist, 1960; Csanady, 1978).

6. The surface sublayer

The major difference between a solid wall and the water side of a free surface is found near the surface. A nearly constant velocity gradient characterizes the velocity distribution here to depths of order 5 cm (at moderate wind speeds $u_* \sim 1$ cm s^{-1}). A typical velocity defect distribution is shown here in Fig. 3. The linear portion of the velocity distribution is, in a sense, the equivalent of a viscous sublayer, except that the velocity gradient is much smaller. The effective surface viscosity,

$$\nu_e = u_*^2 \left|\frac{du}{dz}\right|_s^{-1}, \tag{5}$$

is typically 1 cm^2 s^{-1} and greater in moderate winds, at least two orders of magnitude greater than the molecular viscosity of water. The low observed surface velocity gradient may be confidently ascribed to the stirring action of breaking and sharp crested wavelets.

Upon integrating Eq. (4) one arrives at the familiar logarithmic law:

$$\frac{u}{u_*} = \frac{1}{\kappa}\ln\frac{z}{r} + 8.5 = \frac{1}{\kappa}\ln\frac{z}{z_0}, \tag{6}$$

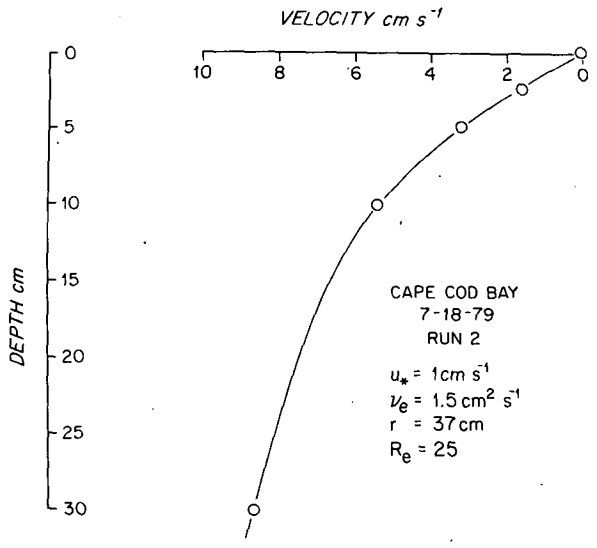

FIG. 3. Typical near-surface velocity defect distribution; data from Churchill and Csanady (1983).

where r is equivalent sand grain roughness and z_0 the alternative roughness length commonly used in meteorology. Either of these parameters characterize the effect of near surface turbulence on the position of the logarithmic line in a $u(\ln z)$ diagram. Physically, this effect consists of more or less efficient stirring, the more efficient, the less the nondimensional velocity u/u_* at a given depth, and the greater the inferred roughness parameter. Although both r and z_0 have the physical dimension of length, it is not very helpful to think of r or z_0 as physical lengths, related perhaps to wavelet amplitude. Over a solid surface the value of the roughness parameter also depends on stability, the presence of a drag-reduction polymer, while over a flexible surface a variety of other influences enter; for further discussion see Csanady (1978). Generally, the roughness parameter is increased by energy supply to the near-surface turbulence, reduced by energy drain, e.g., due to a stable density distribution. Because at a wind blown sea surface there is direct energy supply to the breaking wavelets, a relatively large roughness parameter may be expected on this basis.

The observations show r to be in the range 0.2–2 m and more, i.e., relatively very large. A less puzzling way to express this effect is to say that the nondimensional velocity defect $(u_s - u)/u_*$ is much less at a given depth than it would be over a comparable rough surface, or for that matter, at the same height *above* the sea surface rather than below. The aerodynamic roughness (r or z_0) of the *air side* of the interface at moderate wind speeds is less by a factor of 10–100 than of the water side, although evidently associated with the very same wavelets.

A useful way to illustrate changes of roughness is to show velocity distributions in the universal coordinates of the smooth law of the wall (Monin and Yaglom, 1971). For the free surface shear layer this means a semilogarithmic representation of the form:

$$\frac{u_s - u(z)}{u_*} = \text{func}\left(\ln \frac{u_* z}{\nu}\right). \tag{7}$$

Typical results from observations off Shinecook Inlet, Long Island, in Cape Cod Bay and on Lake Huron are shown in such a diagram in Fig. 4. A somewhat less reliable observation at the so-called "Deep Water Dumpsite," DWD 106, off New York, is also shown. A velocity profile has been added from Bye (1965) (Lough Nead), and one from Kenney (1977) (Lake of the Woods). A similar diagram for a variety of rough solid walls was given many years ago by Van Driest (1956).

All of the free surface shear layer velocity profiles determined in these field studies have a similar general character and differ from the smooth wall layer distribution in that:

1) The velocity defect $(u_s - u)$ just below the surface sublayer, i.e., where the logarithmic law just begins to hold, is only about $3u_*$, or much less than above a sublayer over a smooth solid surface (which is about $10u_*$).

2) At a fixed value of $u_* z/\nu$ the velocity defect $(u_s - u)$ is less by some 10–$20u_*$ than it would be above a smooth surface.

Laboratory observations of Wu (1975, 1983) also showed a relatively thin linear-profile sublayer, and greater roughness on the water than on the air side, although not as great a difference as found in the field.

From the eddy viscosity, friction velocity and roughness length, a Reynolds number may be formed:

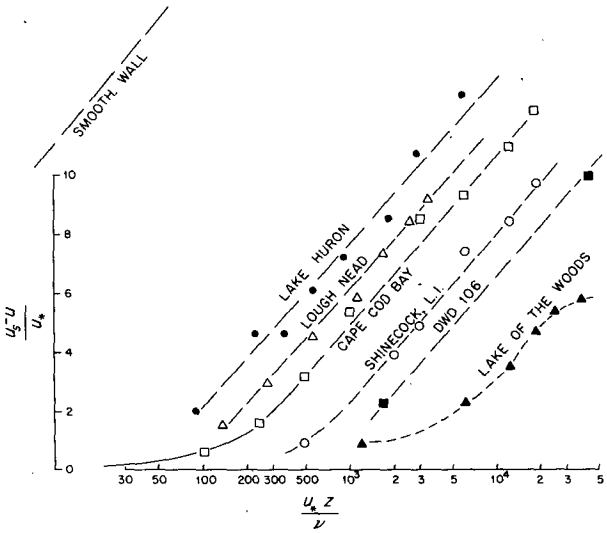

FIG. 4. Typical velocity distributions in different experimental studies in universal law of the wall coordinates. Lough Nead data are from Bye (1965), Lake of the Woods data from Kenney (1977), Cape Cod and Lake Huron data from Churchill and Csanady (1983).

$$\mathrm{Re} = \frac{u_* r}{\nu_e}. \tag{8}$$

The values of Re derived from the various observations scatter somewhat. In our own observations (Churchill and Csanady, 1983) the scatter was, however, well within the observational error, and a realistic mean value was

$$\mathrm{Re} = 22. \tag{9}$$

The constancy of Re suggests that, given the velocity scale u_*, the same length scale determines r and ν_e.

The various quantitative parameters derived from the distributions shown in Fig. 4 are compared in Table 1. Because the observations have not been corrected for Stokes drift, both ν_e and r are underestimates, although they should have the correct order of magnitude.

7. Conclusion

The observational evidence can clearly be interpreted in the framework of the wall layer analogy in a self-consistent manner. This was concluded by many earlier investigators from the character of the mean velocity distribution, and also by Jones and Kenney (1977) from information on turbulent velocity fluctuations. The contrary conclusion of Bye (1967) in his reanalysis of the Lough Nead data rests on a linear calculation of Stokes drift from the wave spectrum. The necessary large near-surface velocity gradient arises in such a calculation from the high wavenumber components of the spectrum, which are not realistically regarded as irrotational, sinusoidal waves.

This and other misleading notions (e.g., on a viscous sublayer) are avoided if one faces the question, in what coordinate system the wall layer analogy should be expected to apply. By defining the sea surface as that produced by the nearly irrotational components of the wave field a clear separation arises between wave motion (which includes Stokes drift), shear flow plus Langmuir circulations, and small-scale turbulence in accordance with the extensive theoretical framework recently constructed by Craik and Leibovich.

Treated in this manner, the free surface shear layer is found to be analogous to the wall layer, characterized by a logarithmic velocity distribution, and Karman's constant the same as over a solid surface. However, presumably because of direct energy input to the small scale surface turbulence by wind, the roughness parameter on the water side becomes much larger than on the air side. Expressed in a more direct manner, the velocity gradients in the free surface shear layer are much smaller than in a wall layer over a solid surface, under otherwise comparable conditions. This is an important result for such practical applications as, for example, oil spill trajectory forecasting.

TABLE 1. Typical quantitative parameters describing free surface shear layer in different experimental studies (shown in Fig. 4).

	u_* (cm s^{-1})	r (cm)	ν_e (cm^2 s^{-1})	Re
Lake Huron	0.9	20	1.1	17
Lough Nead	1.1	23	1.1	23
Cape Cod Bay	1.0	40	1.5	27
Shinecock, L.I.	1.0	115	5	23
DWD 106	0.85	250	—	—
Lake of the Woods	1.2	310	14	27

Acknowledgments. This work was supported by the Department of Energy under a contract entitled "Coastal-Shelf Transport and Diffusion."

APPENDIX

Notes on the Character of a Wind-Blown Sea Surface

Returning to Boston on a cruise ship from Puerto Rico early in March 1973, we had a brisk following wind (10 m s^{-1}) and it so happened that the main wind waves and the ship travelled together almost accurately. This provided a particularly favorable opportunity to observe the wind-blown sea surface, because the eye was able to focus on a single large wave for a long period. Such a wind-blown surface is generally described as chaotic, and this would have been a fair overall characterization also on the occasion mentioned. However, a few distinct types of waves stood out from the total pattern, and by watching this pattern for a longer period one could discern an unexpected degree of order in the chaos.

The main wind waves were fairly regular, one or two meters in amplitude, travelled at a speed of about 10 m s^{-1} (the known speed of the ship) and had a wavelength of the order of the theoretical deep-water value of 20π m. On this large scale, fast moving undulation there were superimposed three kinds of short, slowly moving wavelets:

1) Capillary waves of an estimated wavelength of 0.5 cm.

2) Crescent-shaped capillary-gravity waves of a wavelength (along wind) of order 0.3 m, illustrated in Fig. 4.

3) As 2), but of somewhat greater wavelength, order 1 m.

Types 1) and 2) were ubiquitous, but denser and larger on the rising (windward) side of the large waves. Together, they created an "old man's skin" look with many wrinkles. Larger type 3) crescents were present only on the rising windward face of the large waves. Many of the crescents broke at their leading edge, usually when they were near the top of a large wave. The coalescence of a number of little (crescent) whitecaps sometimes created a larger whitecap. In the troughs

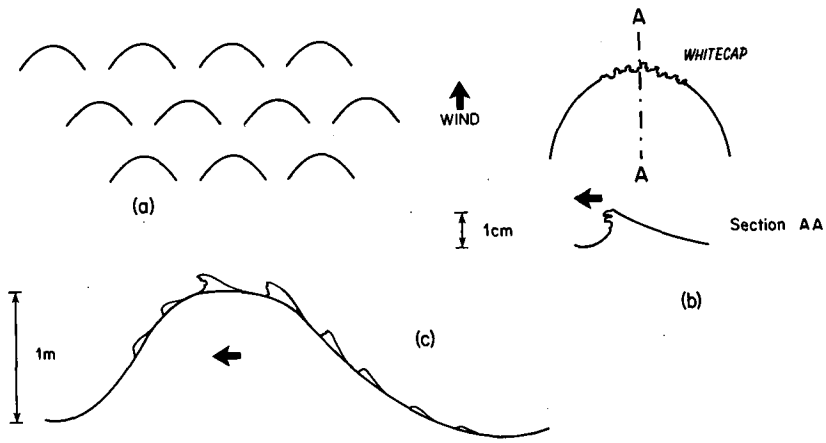

FIG. 5. Schematic illustration of wavelets observed on sea surface: (a) horizontal plan of crescent-shaped capillary gravity wavelets, (b) individual wavelet detail in plan and cross section, (c) section through main wind wave showing wavelets.

of the large waves the large crescents disappeared, the smaller ones became much smoother. All the small wavelets being slow, they were raised and lowered by the larger waves and left behind. The back (windward) side of the crescents were slightly hollowed (Fig. 5) and seemed to be acting as so many little "sails", the wind lying into them. When the crescents were lit by the sun on their sharp forward side, their shape was brightly outlined on the background.

When an especially strong gust of wind passed, the surface responded instantly and became rougher (i.e., the capillary waves and crescents became larger and more numerous), in much the same way as the surface on the rising side of a large wave in each wave cycle, only more so. I put down in my notes that the sea surface was evidently an excellent instantaneous stress meter, an idea that has occurred to others before and that has now been exploited in satellite observations (Jones and Schroeder, 1978).

A short distance (perhaps 0.1 m) below the busy surface long straight windrows of sargassum weed could be discerned, with a spacing of some 50 m. The quiescence of these was striking, given the chaos immediately above. The surface was undoubtedly full of small-scale turbulence but this evidently did not penetrate very deep.

There were a number of other, apparently random, irregularities in the surface wave field that did not lend themselves to easy characterization. A Fourier analysis of the surface elevation field would no doubt have yielded a continuous spectrum. Nevertheless, the wavelet types described above were distinct and present over the entire period of observation, i.e., over 48 h of steady following wind. The crescent-shaped wavelets of order 0.3 m wavelength can also be observed on wind-blown ponds on Cape Cod, where I have watched them many times.

REFERENCES

Bye, J. A. T., 1965: Wind-driven circulation in unstratified lakes. *Limnol. Oceanogr.*, **10**, 451–458.

——, 1967: The wave drift current. *J. Mar. Res.*, **25**, 95–102.

Chang, M. S., 1969: Mass transport in deep-water long-crested random gravity waves. *J. Geophys. Res.*, **74**, 1515–1536.

Churchill, J. H., and G. T. Csanady, 1983: Near-surface water velocity measurement using acoustically and visually tracked drogues. In the press, JPO.

Craik, A. D. D., 1970: A wave-interaction model for the generation of windrows. *J. Fluid Mech.*, **41**, 801–821.

——, 1977: The generation of Langmuir circulations by an instability mechanism. *J. Fluid Mech.*, **81**, 209–223.

——, 1982: The drift velocity of water waves. *J. Fluid Mech.*, **116**, 187–205.

——, and S. Leibovich, 1976: A rational model for Langmuir circulations. *J. Fluid Mech.*, **73**, 401–426.

Csanady, G. T., 1963: Turbulent diffusion in Lake Huron. *J. Fluid Mech.*, **17**, 360–384.

——, 1965: Windrow studies. Rep. No. PR26, Great Lakes Institute, University of Toronto, 82 pp.

——, 1970: Dispersal of effluents in the Great Lakes. *Water Res.*, **4**, 79–114.

——, 1978: Turbulent interface layers. *J. Geophys. Res.*, **83**, 2329–2342.

——, and B. Pade, 1969: Windrow observations. *Dynamics and Diffusion in the Great Lakes*, G. T. Csanady, Ed., University of Waterloo, 142 pp.

Donelan, M. A., 1978: Whitecaps and momentum transfer. *Turbulent Fluxes through the Sea Surface, Wave Dynamics and Prediction.* A. Fevre and K. Hasselmann, Eds., Plenum, 273–287.

Ekman, V. W., 1905: On the influence of the earth's rotation on ocean currents. *Ark. Mat. Astron. Fys.*, **2**, 1–52.

Flierl, G. R., 1981: Particle motions in large-amplitude wave fields. *Geophys. Astrophys. Fluid Dyn.*, **18**, 39–74.

Jones, I. S. F., and B. C. Kenney, 1977: The scaling of velocity fluctuations in the surface mixed layer. *J. Geophys. Res.*, **82**, 1392–1396.

Jones, W. L., and L. C. Schroeder, 1978: Radar backscatter from the ocean: dependence on surface friction velocity. *Bound.-Layer Meteor.*, **13**, 133–149.

Kawai, S., 1981: Visualization of airflow separation over wind-wave crests under moderate wind. *Bound.-Layer Meteor.*, **21**, 93–104.

——, 1982: Structure of air flow separation over wind wave crests. *Bound.-Layer Meteor.*, **23**, 503–521.

Kenney, B. C., 1977: An experimental investigation of the fluctuating currents responsible for the generation of windrows. Ph.D. thesis, University of Waterloo, Ontario, 163 pp.

Kenyon, K. E., 1969: Stokes drift for random gravity waves. *J. Geophys. Res.*, **74**, 6991–6994.

Kinsman, B., 1965: *Wind Waves: Their Generation and Propagation on the Ocean Surface.* Prentice-Hall, 676 pp.

Kondo, J., Y. Fujinawa and G. Naito, 1973: High-frequency components of ocean waves and their relation to the aerodynamic roughness. *J. Phys. Oceanogr.*, **3**, 197–202.

Kraus, E. B., 1972: *Atmosphere–Ocean Interaction.* Clarendon, 275 pp.

Leibovich, S., 1977: On the evolution of the system of wind drift currents and Langmuir circulations in the ocean. Part I: Theory and the averaged current. *J. Fluid Mech.*, **79**, 715–743.

——, 1980: On wave–current interaction theories of Langmuir circulations. *J. Fluid Mech.*, **99**, 715–724.

——, 1983: The form and dynamics of Langmuir circulations. *Annual Review of Fluid Mechanics*, **15**, Annual Reviews, 391–427.

——, and S. Paolucci, 1980: The Langmuir circulation instability as a mixing mechanism in the upper ocean. *J. Phys. Oceanogr.*, **10**, 186–207.

——, and ——, 1981: The instability of the ocean to Langmuir circulations. *J. Fluid Mech.*, **102**, 141–167.

Lofquist, K., 1960: Flow and stress near an interface between stratified liquids. *Phys. Fluids*, **3**, 158–175.

Longuet-Higgins, M. S., 1953: Mass transport in water waves. *Phil. Trans. Roy. Soc. London*, **A245**, 535–581.

——, 1960: Mass transport in the boundary layer at a free oscillating surface. *J. Fluid Mech.*, **8**, 293–306.

——, and J. S. Turner, 1974: An "entraining plume" model of a spilling breaker. *J. Fluid Mech.*, **63**, 1–20.

Madsen, O. S., 1977: A realistic model of the wind-induced Ekman boundary layer. *J. Phys. Oceanogr.*, **7**, 248–255.

——, 1978: Mass transport in deep-water waves. *J. Phys. Oceanogr.*, **8**, 1009–1015.

Monin, A. S., and A. M. Yaglom, 1971: *Statistical Fluid Mechanics.* MIT Press, 769 pp.

Munk, W. H., 1955: High frequency spectrum of ocean waves. *J. Mar. Res.*, **14**, 302–314.

Neumann, G., and W. J. Pierson, 1966: *Principles of Physical Oceanography.* Prentice Hall, 545 pp.

Phillips, O. M., 1966: *The Dynamics of the Upper Ocean.* Cambridge University Press, 261 pp.

Pierson, W. J., 1962: Perturbation analysis of the Navier-Stokes equations in Lagrangian form with selected linear solutions. *J. Geophys. Res.*, **67**, 3151–3160.

Roll, H. U., 1965: *Physics of the Marine Atmosphere.* Academic Press, 426 pp.

Rossby, C.-G., and R. B. Montgomery, 1935: The layer of frictional influence in wind and ocean currents. *Pap. Phys. Oceanogr. Meteor.*, **3**, 101 pp.

Shemdin, O. H., 1972: Wind-generated current and phase speed of wind waves. *J. Phys. Oceanogr.*, **2**, 411–419.

Ünlüata, Ü., and C. C. Mei, 1970: Mass transport in water waves. *J. Geophys. Res.*, **75**, 7611–7618.

Van Driest, E. R., 1956: On turbulent flow near a wall. *J. Aeronaut. Sci.*, **23**, 1007–1011.

Weber, J. E., 1983: Steady wind- and wave-induced currents in the open sea. *J. Phys. Oceanogr.*, **13**, 524–530.

Wu, J., 1969: Wind stress and surface roughness at air–sea interface. *J. Geophys. Res.*, **74**, 444–455.

——, 1975: Wind induced drift currents. *J. Fluid Mech.*, **68**, 49–70.

——, 1983: Viscous sublayer below wind-disturbed water surface. (In preparation.)